Piotr DUKALSKI
Bartłomiej BĘDKOWSKI
Krzysztof PARCZEWSKI
Henryk WNĘK
Andrzej URBAŚ
Krzysztof AUGUSTYNEK

DYNAMICS OF THE VEHICLE REAR SUSPENSION SYSTEM WITH ELECTRIC MOTORS MOUNTED IN WHEELS

DYNAMIKA UKŁADU TYLNEGO ZAWIESZENIA POJAZDU Z SILNIKAMI ELEKTRYCZNYMI WBUDOWANYMI W KOŁA*

The dynamics analysis of the rear suspension system of the Fiat Panda III with electric motors mounted in wheels is presented in the paper. The simplified model of this system modeled using the multibody system dynamics method and the MSC. Adams package is proposed. In order to validate the proposed numerical model, the road tests were carried out consisting on passing the vehicle without motors in wheels at constant speed through the obstacle. The vertical displacement of the center of the vehicle wheel was measured during the tests. During the validation, parameters of the wheel-to-road contact, stiffness coefficients of springs and shock absorber damping coefficients of the suspension of the simulation model were modified so that the numerical results were consistent with the experiment. Further, such a tuned model was used to simulate the motion of suspension with the motors mounted into the wheels. The obtained results were validated, obtaining the accepted compatibility. In the following, a series of calculations was carried out in order to analyze the influence of stiffness coefficients of springs and shock absorber damping coefficients on the dynamic response of the suspension.

***Keywords**: multibody system dynamics, rear suspension system, electric motor, wheel hub motor.*

W artykule przedstawiono analizę dynamiki układu tylnego zawieszenia samochodu Fiata Panda III z silnikami elektrycznymi wbudowanymi w koła. Uproszczony model układu uzyskano przez zastosowanie metod dynamiki układów wieloczłonowych i ich implementacji programowej w postaci pakietu MSC.Adams. W celu walidacji zaproponowanego modelu symulacyjnego wykonano testy drogowe polegające na przejeździe pojazdu bez silników wbudowanych w koła przez przeszkodę ze stałą prędkością. Podczas badań mierzono pionowe przemieszczenia środków kół pojazdu. W procesie walidacji modyfikowano parametry kontaktu koła z nawierzchnią, współczynniki sztywności sprężyn zawieszenia oraz współczynniki tłumienia amortyzatorów, tak aby otrzymać akceptowalną zgodność wyników numerycznych z eksperymentem. Dostrojony model symulacyjny został dalej użyty do symulacji ruchu zawieszenia z silnikami wbudowanymi w koła. Otrzymane wyniki dalej porównano z badaniami uzyskując akceptowalną zgodność. W pracy wykonano również szereg symulacji mających na celu zbadanie wpływu współczynników sztywności sprężyn zawieszenia i współczynników tłumienia amortyzatorów na odpowiedź dynamiczną układ tylnego zawieszenia.

***Słowa kluczowe**: dynamika układu wieloczłonowego, układ tylnego zawieszenia, silnik elektryczny, silnik w piaście koła.*

1. Introduction

Almost a quarter of carbon dioxide (CO_2) emissions come from transport, and urban mobility accounts for 40% of all carbon dioxide emissions from road transport. Transport is particularly vulnerable to disruptions in oil supplies and instability of its prices. Therefore, the growing concerns about the security of energy supply the awareness of climate change and the increase in the health awareness of the public cause the transition from fossil fuels to alternative fuels. The regulations of the European Union force the ever-increasing share of low or "zero-emission" vehicles used in cities. Energy-efficient vehicles play an important role in the energy and climate policy, and electromobility has been recognized as one of the priorities for Europe. All

activities carried out in this direction are connected with the creation of a number of construction solutions for electric vehicle drive systems [2, 3, 9].

The article presents possible solutions for drive systems of electric vehicles, describing their advantages and disadvantages. A model for simulating the work of the car suspension with mounted two electric motors in the wheel hubs was presented. This solution, due to the increase of unsprung masses, may cause a deterioration of comfort of travel, which caused that the problem of vertical vibrations of the suspension was addressed. Some examples of the solutions and challenges associated with in-wheel motor integration have been presented by Watts, Vallance et al. [16].

The transmission of vibrations resulting from the unevenness of the road to passengers has a major impact on passenger comfort, efficiency and health. Comfortable driving increases passenger satisfaction [4, 15]. For this reason, vehicle manufacturers care about the comfort of traveling. The use of electric drive motors in the wheels affects the mass increase of the unsprung vehicle and this can affect the comfort of traveling. A similar range of analyzes is presented by Anderson and Harty [1]. The transmission of vibrations to passengers is related to the height of the road unevenness and the stiffness and damping of the vibrations by the suspension of the wheel. Vibrations with frequencies up to 12 Hz affect all human organs, while vibrations above 12 Hz have local effects [17]. Low frequencies (4, 6 Hz) generated by cyclic movements, caused by tires rolling on uneven roads, can cause resonance. Prolonged exposure to vibrations increases muscle fatigue and makes the user will be more susceptible to spinal injuries.

In the further part of the article there is a dynamic analysis of the vehicle rear suspensions with electric motors mounted in the wheels of the vehicle. Simulation studies of the solution with motors in wheels and compare with vehicle without motors in wheels were carried out. The results of the simulations were verified with the experimental tests.

2. Solutions for drive systems of electric vehicles

In electric vehicles, many configurations of drive systems are used, ranging from the closest to vehicles powered by an internal combustion engine - replacement of the internal combustion engine by an electric motor, successively reducing the components of the classical vehicle's propulsion system, to the solution where the motors separately drive the left and right wheels of the vehicle [12]. Fig. 1 shows schematically the individual solutions of drive systems.
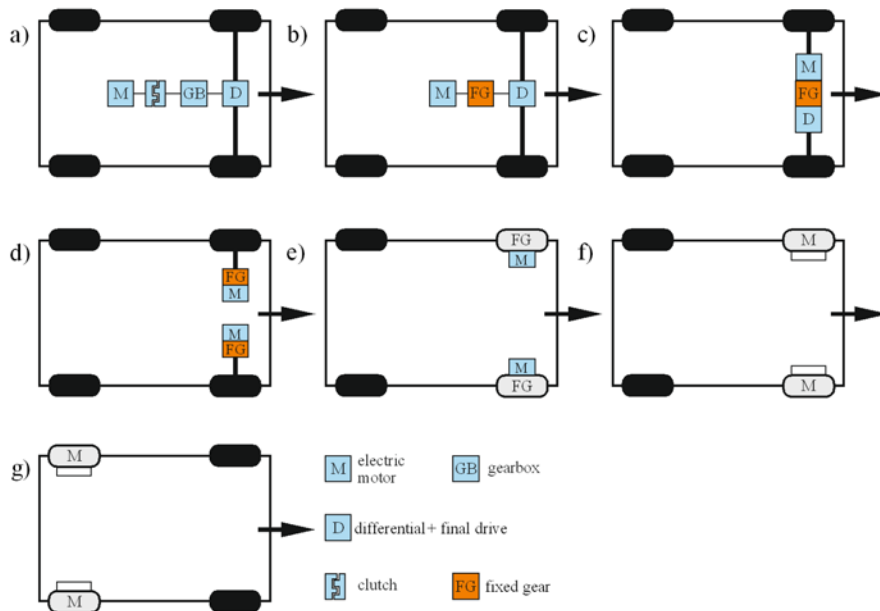

Fig. 1. Configurations of the electric drive system

The advantage of the first solution (Fig. 1a) is the possibility of using an internal combustion engine or an electric motor, alternatively. The disadvantage is to leave all the components of the classic drive system. In the case of the second and third solutions (Fig. 1b), the advantage is to relinquish the clutch and gearbox to a fixed gearbox, which reduces the system weight and reduces production costs. The disadvantage may be the speed limit of the vehicle resulting from the maximum speed of the electric motor. The solution shown in Fig. 1c differs from the previous by transverse engine placement. Another solution (Fig. 1d) shows the system in which the differential mechanism was skipped. This allowed the use of two motors with lower power driving the right and left wheels individually. The use of this solution requires the control of the rotational speed of the motors during cornering or braking [5, 6]. In this case the drive torque on the wheels is transmitted via the axle shaft and therefore the unsprung masses do not change. In the case of solutions shown in the following drawings: a motor with a gear with constant ratio (Fig. 1e) or without it (Fig.1f), it is mounted in the wheel of the vehicle. Modification of the solution shown in Fig. 1f (motors are mounted in the front wheels) drive motors may be the assembled in the rear wheel hubs (Fig. 1g). The advantages of this solution are: considerable simplification of the propulsion system, resignation of mechanical transmissions, leaving space between the wheels of the vehicle to use. The disadvantages are: increasing the unsprung vehicle mass, the need to vary the speed of the wheels when cornering and braking, limiting the size of the motor to the inner part of the wheel with leaving space for the brake.

Taking into account the advantages and disadvantages of this solution, the dynamics of the rear suspension of the vehicle with built-in electric motors were analyzed. Tests and analyzes were carried out to determine the changes of accelerations and amplitudes acting on the rear axles and vehicle body (in the area of passenger seats). To this reason was developed the rear suspension simulation model using the MSC. Adams package. This model was verified on the basis of the test results of the actual car, in which on wheels and suspension, additional masses corresponding to the rotating and immobile elements of electrical motors used for driving and braking the wheel were mounted. The evaluation of the suspension dynamics using a quarter-car simulation with an in-wheel motor integration and comparison it to the solution propulsion with internal combustion engine has been presented in [11, 15].

The article does not include the analysis of the movement of the wheel in case of application of the driving / braking torque, only the vertical vibrations of the freely rotating wheel were taken into account.

Comparative tests of the vehicle with mounted electric motors in the wheels and without them were carried out. Vertical dynamics tests of suspension were carried out in time and frequency analysis. The comparison was based on the root mean square *RMS* and the vibration dose values *VDV* in time.

Root Mean Square (*RMS*) and Vibration Dose Values (*VDV*)

The *RMS* method calculates the value of acceleration by the square root of the mean value obtained from the integration of the square value of the signal. In the case of a signal containing a sharp vibration jump *RMS* increases rapidly during each of these events, but also decreases with increasing averaging time.

In the event that the vertical movement of the vehicle suspension changes in a step-wise manner or is generated by a single pulse, the *VDV* vibration is well-suited for analysis. It is considered a good indicator, especially for signals with high dynamics. It allows you to measure the total vibration exposure, taking into account the size, frequency and duration of the exposure. The *VDV* determines the total vibration exposure in a given period of time.

The weighted *RMS* and *VDV* acceleration are expressed by means of the following formulas:

$$RMS = \sqrt{\frac{1}{t}\int_0^t a_z^2 dt}, \qquad (1)$$

$$VDV = \sqrt[4]{\int_0^t a_z^4 dt}, \qquad (2)$$

where: a_z weighted mean acceleration and t is the measurement time [8].

If the VDV is smaller than 8.5, the ISO 2631-1[19] standard them as low, the impact on human health have not been clearly documented. When VDV values are in the range of 8.5-17 the ISO 2631-1 standard defined them as moderate for which caution with respect to potential risk is indicated and for VDV values higher than 17 it defined in the ISO standard as high, health risk are likely.

3. Construction of the electric motor assembled in w wheel

The vehicle drive is equipped with two traction electric motors mounted into the wheel hubs. These motors are manufactured in the Institute of Electrical Drives and Machines **KOMEL** (Fig. 2). They are synchronous motors, excited with permanent magnets. The overall dimensions of the developed motor have been adapted to the 17" wheel rim.

The presented motor is an electric motor with an external rotor. The rotating element is a hull that performs the function of a rotor, in which the magnetic

Fig. 3. The 3D model of the SMZs200S32 electric motor - KOMEL

core is mounted with fixed permanent magnets. The fixed element is an anchor disc with a supporting structure, a labyrinthine cooling system and a stator made up of a coiled magnetic core.

The construction of the motor is limited by the outer diameter, shape and shoulder of the tyre, and the brake drum (Fig. 3).

The motor components can be divided into fixed parts and movable parts, through which the torque is transferred directly to the vehicle wheel. A rotor position sensor is necessary to control the motor.
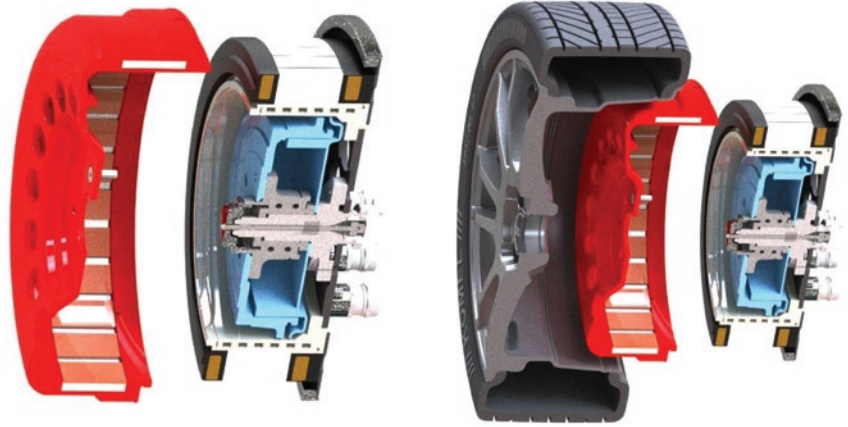
The motor has an incremental encoder as standard.

The parameters of the electric motor are presented in Tab. 1. The motor is mounted to the beam through the anchor disc (Fig. 4).

The drive system equipped with two motors of this type should ensure dynamic driving of the Fiat Panda III. For vehicles with a larger weight, in order to obtain a suitably high driving parameters, a drive with four motors should be used.

4. Experimental research

The authors set out to investigate the vertical movement of the rear suspension of the vehicle while overcoming a single obstacle of a road with a relatively high altitude. They may occur while passing through rail rails, craters in the road, or small objects lying on it. Similar vibrations will occur when overcoming the speed bump [13, 18]. Two different obstacles were deliberately used, one with a triangular shape, generating a movement of the wheel upwards and then downwards and a rectangular one, at which the vertical movements of the wheel are separated to each other (Fig. 5). For determining the dimensions of obstacles, the limit values of inequalities on roads determined by Kropáč and Múčka [10] were used.

4.1. Description of research

A B Class passenger car was used in the tests, in which measuring equipment was installed (shown in Fig. 6), allowing for measurements of wheel axle distance from the roadway (1), suspension deflections (2), driving speed (3), accelerations acting on the wheel axle (4) and the vehicle body directly above the wheel axle (5) and rotational speed of the wheel (6). The results were recorded on the memory disk of the measuring apparatus with recording frequency 100 Hz [14]. The tire pressures were in accordance with the vehicle manufacturer's recommendations and they were the same in both case, with masses simulating the electric motors in the wheels and without them.

Fig. 2. The real model of the SMZs200S32 electric motor - KOMEL

Table 1.   Parameters of electric motor

Parameter	Value
line to line voltage U_{LL}, V	200
nominal power P_n, kW	42
nominal torque M_n, Nm	400 (for $n_n = 0 \div 1000\,\mathrm{obrmin}^{-1}$)
max. power P_{max}, kW	~ 80
max. torque M_{max}, Nm	~ 900 (for $n_n = 0 \div 850\,\mathrm{obrmin}^{-1}$)

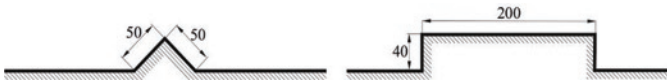Fig. 4. The 3D model of assembly of the SMZs200S32 electric motor - KOMEL

Fig. 5. Obstacles used for tests

Fig. 6. Test object with mounted measuring apparatus

4.2. Methodology of carrying out measurements

The measurements were carried out on a flat, horizontal roadway section. For comparison, obstacle in the shape of a triangular was chosen - an *L50* triangular(which corresponds to an unevenness of 44 mm with a base length of 85mm) and a rectangular one with a height of 44mm and a length of 200 mm. The obstacle was crossed by at a speed of ~12kmh^{-1}. With this car's speed of movement and

the length of unevenness, the frequency of excitations caused by road unevenness will be in the range of 1-3 Hz. This is the amplification range of the amplitude of the vertical vibrations of the suspension. At higher velocities, the amplitude of vertical vibrations will be strongly suppressed, which will reduce the effect of increasing the unsprung mass acting on the vehicle body and passengers. Fig. 7 shows the moment of entering the wheel with an obstacle of a rectangular.

The tests were carried out in two mass configurations: standard vehicle and with additional masses simulating the presence of electric motors. These masses correspond to the mass of the rotor and the stator of the drive. It is assumed that the stiffness of the suspension spring and damping coefficient of the shock absorber are the same for both configurations. These parameters are further used during the validation of the simulation model of the rear suspension system.

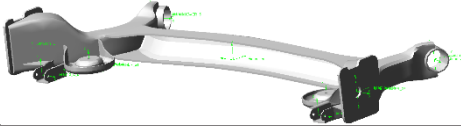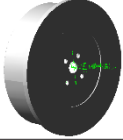### 5. Multibody model of the rear suspension system

The Autodesk Inventor package was used to model the rear vehicle suspension system with the engine mounted into the wheel, dedicated to creating 3D subassembly models. The MSC.Adams package was used to analyze the dynamics. In Tab. 1 lists the parts used in the model together with their mass parameters. Most of the parts listed in the table represent the mapping of real elements. The only exception is the stator and rotor, whose mass parameters have been chosen so that they reflect the components of the electric motors in them. For some parts, simplifications have been applied, such as removing the grooves in the tire or eliminating rounding and chamfers for other parts. All these changes have no major influence on the results of the dynamics simulation, and only facilitate the import of the models so made to the MSC.Adams package.

The shock absorber is modeled as a spring-damping element whose first attachment point is located in the suspension beam, while the second one is treated as a virtual point associated with the mainstay (Fig. 8). The coordinates of the second point result from its location in the vehicle body, which is not modeled in the model of the rear suspension. These coordinates have been determined on the basis of

Fig. 7. View of overcoming road unevenness by the vehicle's wheel

Table 2. Mass parameters of parts of the rear the suspension system

Name of the component	mass [kg]	mass moment of inertia [kgm^2]		
	m	I_x	I_y	I_z
suspension beam	20.2	4.7725	4.4934	0.3407
stator	24	0.5418	0.2999	0.2997
axle shaft	1.4	$1.4663 \cdot 10^{-3}$	$1.2233 \cdot 10^{-3}$	$1.1155 \cdot 10^{-3}$
wheel disk	1.9	$1.7616 \cdot 10^{-2}$	$9.1581 \cdot 10^{-3}$	$9.1406 \cdot 10^{-3}$
brake drum	5.3	$5.3173 \cdot 10^{-2}$	$2.8430 \cdot 10^{-2}$	$2.8430 \cdot 10^{-2}$
rotor	12	0.3694	0.1989	0.1988
rim	8.9	0.2822	0.1681	0.1676
tire	7	1.1403	0.6383	0.6382

available car documentation. In the case of the spring, the value of the damping coefficient is equal to zero. A similar approach is applied to the shock absorber with the difference that here a non-zero value of the damping coefficient is assumed and the stiffness coefficient is equal to zero.

The contact element between the tire and road has been introduced. Because, the vehicle moves with a constant speed in a straight line, a standard contact model has been adopted.

The contact parameters are presented in Tab. 4.

The stiffness coefficient of spring (1.8×10^4Nm^{-1}), the shock absorber damping coefficient (2.4×10^3Nsm^{-1}) and contact parameters of road-wheel were validated in the numerical model by means of experimental results for the vehicle without motors in wheels.

The multibody system dynamics model of the rear suspension system is presented in Fig. 9.

In order to take into account the weight of the vehicle body, two concentrated masses (180kg) were added to the model.
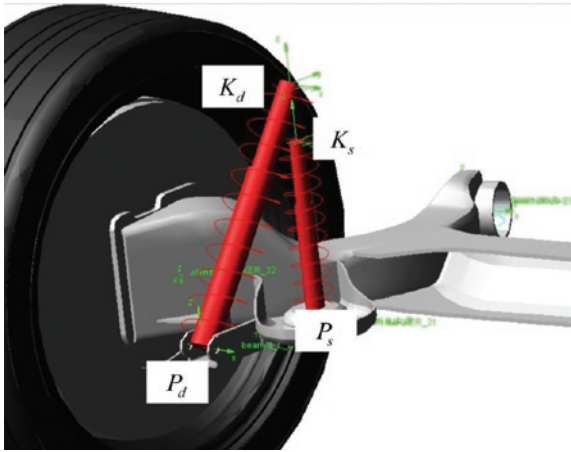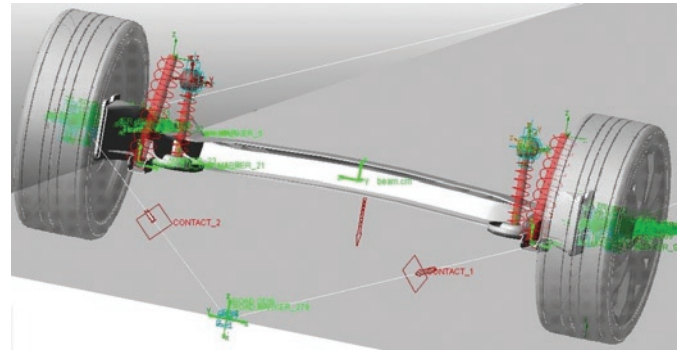
Fig. 8. View of spring and shock absorber

Fig. 9. Multibody system of the rear suspension system

6. Numerical calculations and measurement results

Table 3. Parameters of springs and dampers applied in simulations

Parameter	springs		shock absorbers	
	left	right	left	right
global coordinates of point $P_i\big|_{i\in\{s,d\}}$ [m]	$\begin{bmatrix} 0.455 \\ -0.2 \\ 0.006 \end{bmatrix}$	$\begin{bmatrix} -0.455 \\ -0.2 \\ 0.006 \end{bmatrix}$	$\begin{bmatrix} 0.53 \\ -0.315 \\ 0.006 \end{bmatrix}$	$\begin{bmatrix} -0.53 \\ -0.315 \\ 0.006 \end{bmatrix}$
global coordinates of point $K_i\big|_{i\in\{s,d\}}$ [m]	$\begin{bmatrix} 0.455 \\ -0.2 \\ 0.231 \end{bmatrix}$	$\begin{bmatrix} -0.455 \\ -0.2 \\ 0.231 \end{bmatrix}$	$\begin{bmatrix} 0.53 \\ -0.125 \\ 0.271 \end{bmatrix}$	$\begin{bmatrix} -0.53 \\ -0.125 \\ 0.271 \end{bmatrix}$
stiffness coefficients $k_s[\text{Nm}^{-1}]$	$1.2\cdot10^4$ $1.8\cdot10^4$ $2.4\cdot10^4$			
length at preload [m]	0.35			
damping coefficients $c_s[\text{Nsm}^{-1}]$	$1.2\cdot10^3$ $2.4\cdot10^3$ $3.6\cdot10^3$			

Table 4. Parameters of the contact tire-road

Contact parameters	Value
stiffness coefficients k_{tr}, Nm^{-1}	$5.2\cdot10^5$
force exponent δ	1.1
damping coefficients c_{tr}, Nsm^{-1}	$4.8\cdot10^3$
static friction coefficient μ_s	0.8
dynamic friction coefficient μ_d	0.6
stiction transition velocity v_s, ms^{-1}	0.1
friction transition velocity v_f, ms^{-1}	1

The comparison of the results obtained in numerical calculation with these obtained from the experimental set-up is presented in Fig. 10-12. Left figures show displacement (z), velocity (u_z) and acceleration (a_z) of the center of wheel obtained for the rear suspension system in which additional mass in wheels is neglected. Right figures present results obtained for the system with mounted additional mass in wheels. Displacement was measured directly during experiment. These results were interpolated using the cubic spline interpolation. The velocity and acceleration were calculated using central-difference formulas. The Butterworth 4-th order low pass filter was applied to eliminate frequencies higher than 16 Hz from the dynamic response. The highest accelerations can be observed for frequencies lower than 16 Hz. Vibrations excited during passing through an obstacle are also in these ranges. Moreover human discomfort has been proved to be more sensitive for frequencies from 3 to 10 Hz.

It can be observed good compatibility of the results obtained from simulation model with those obtained by experimental measurements. The period and amplitude of oscillations obtained from the simulations are close to those measured.

Figs. 13 and 14 show the frequency domain response of the velocity and acceleration.

It can be seen, that in the case of a vehicle passing through a triangular obstacle in the frequency range considered, the suspension behaves like a system with one degree of freedom. The natural frequency of the system, obtained from the experiment and simulation model, is about 4.5 Hz. In the case of passing through a rectangular obstacle, it can be noticed that an additional frequency of approx. 10 Hz is induced. If an additional unsprung mass is introduced, this frequency disappears, while the first of these frequencies still occurs in the acceleration and velocity spectrum despite the introduced structural changes. It can be seen that the differences between presented courses are not large and do not exceed 5%.

In further considerations influence of the spring stiffness and shock absorber damping coefficient on the dynamic response of the rear suspension system is analysed.

Figs. 15 and 16 show time courses of the wheel centre acceleration obtained from numerical simulations. In Fig. 15 it is assumed that the value of damping coefficient is constant (c=2.4x10³ Nsm⁻¹) and different spring stiffness are applied in simulations. Fig. 16 contains
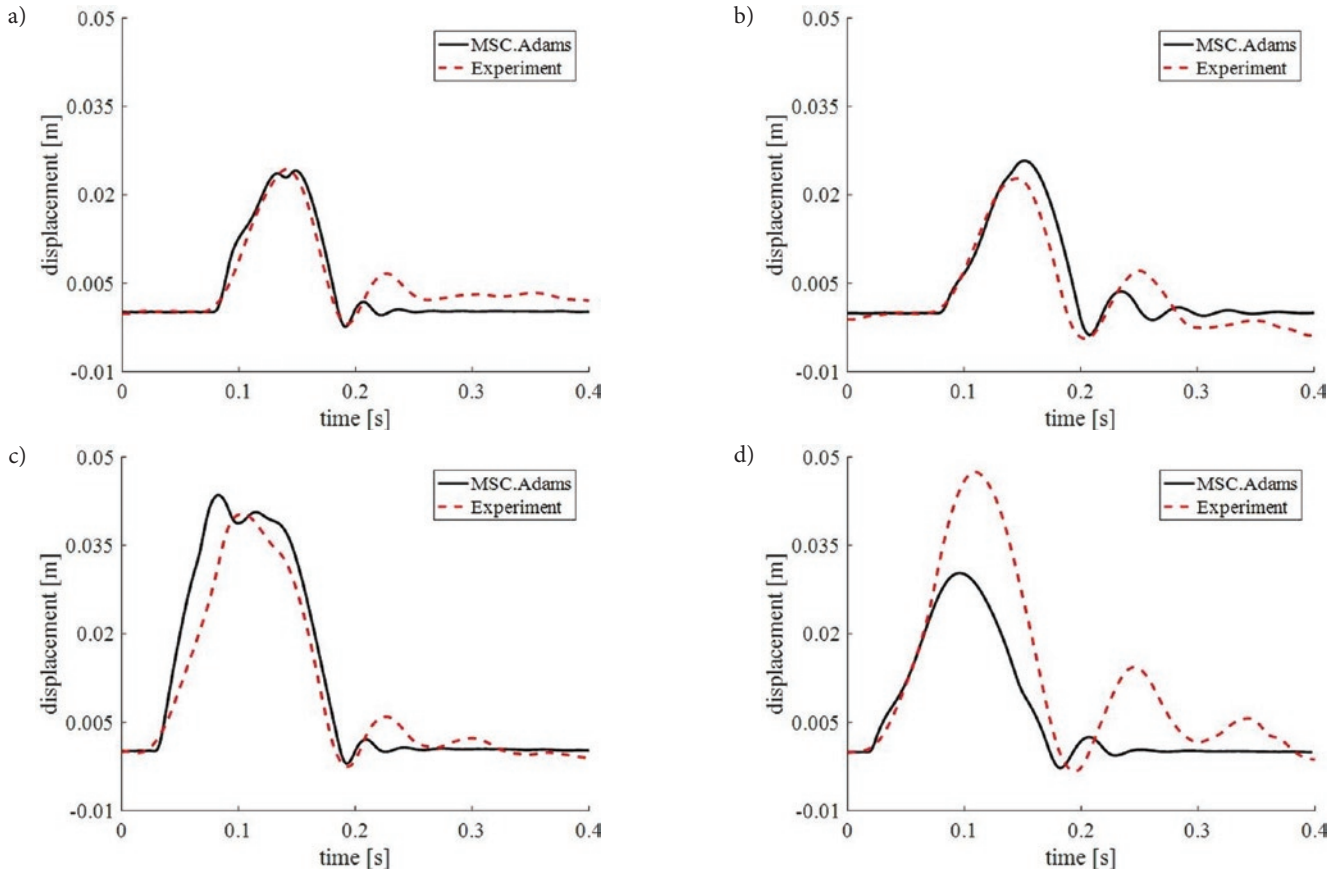
Fig. 10. Vertical displacement of wheel a) and b) triangular obstacle without and with motors c) and d) rectangular obstacle without and with motors
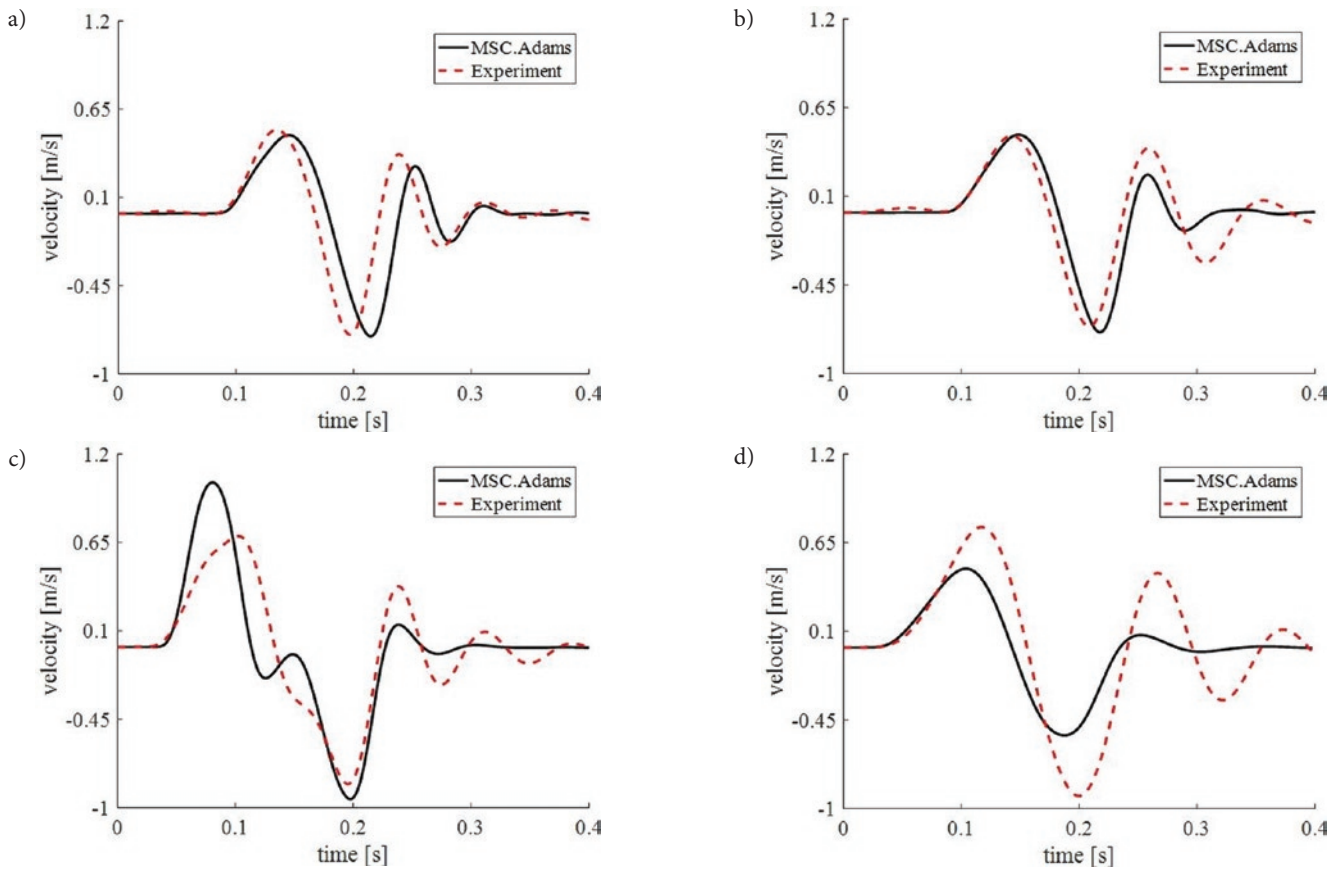

Fig. 11. Vertical velocity of wheel a) and b) triangular obstacle without and with motors c) and d) rectangular obstacle without and with motors
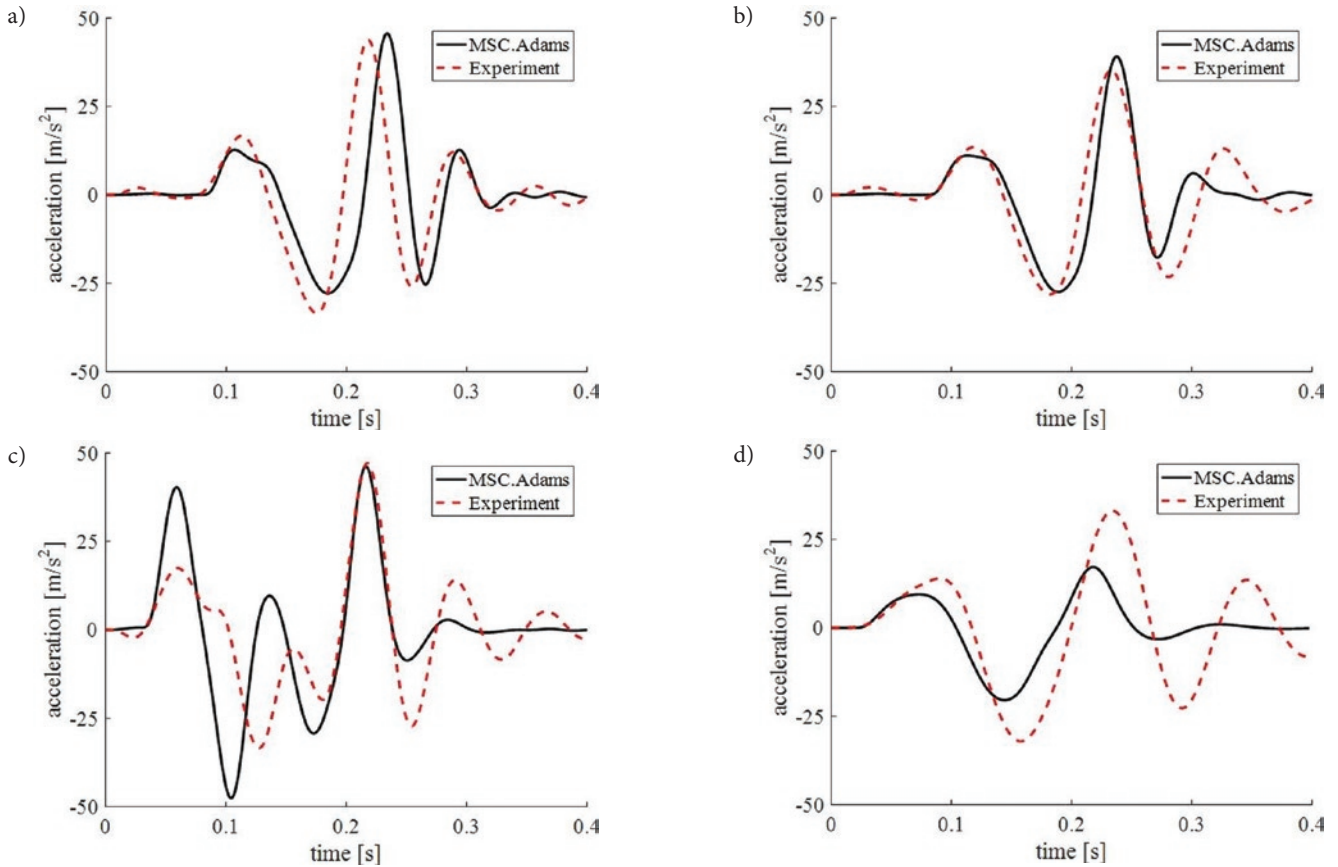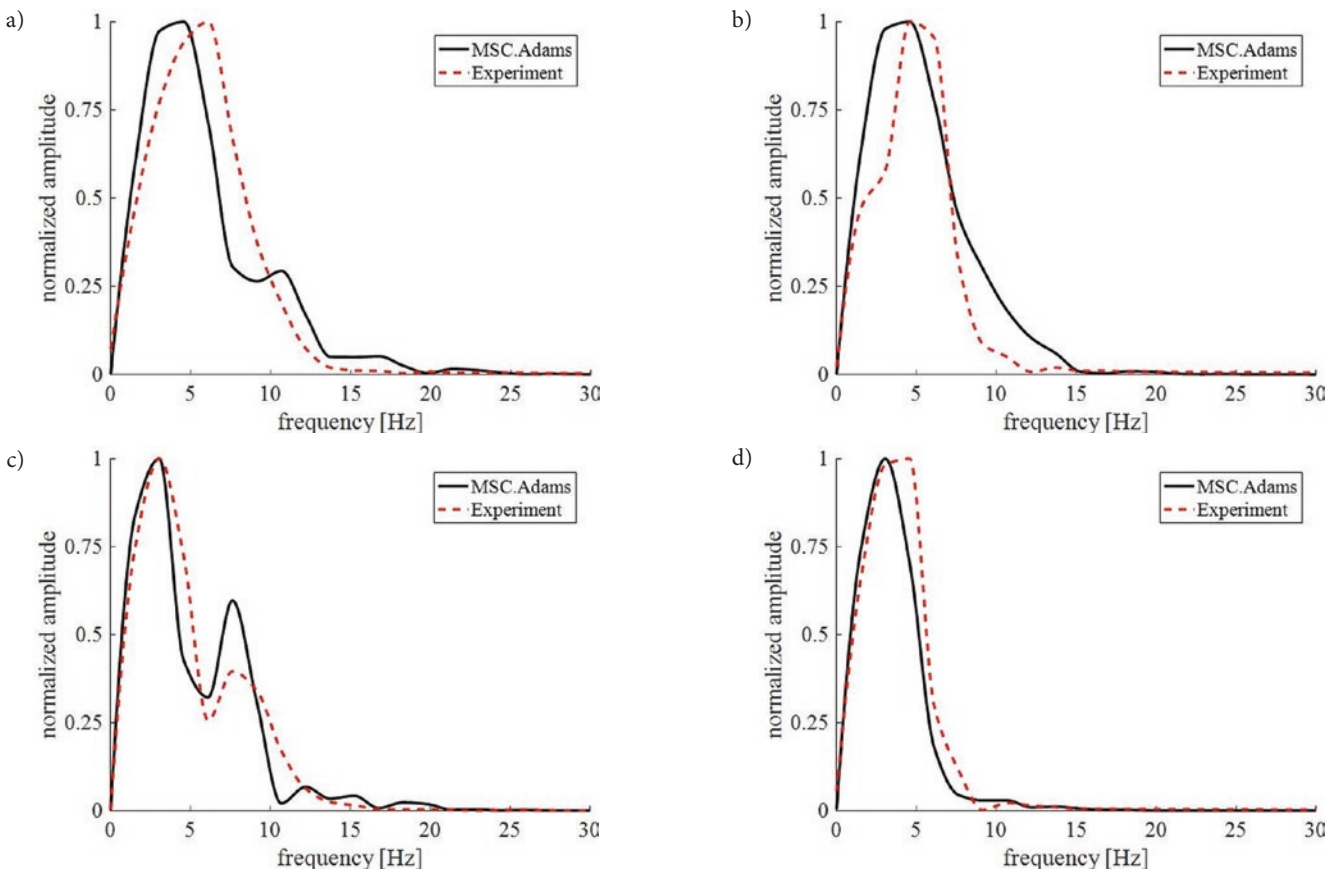
Fig. 12. Vertical acceleration of wheel a) and b) triangular obstacle without and with motors c) and d) rectangular obstacle without and with motors

Fig. 13. Frequency response for velocity of wheel a) and b) triangular obstacle without and with motors, c) and d) rectangular obstacle without and with motors
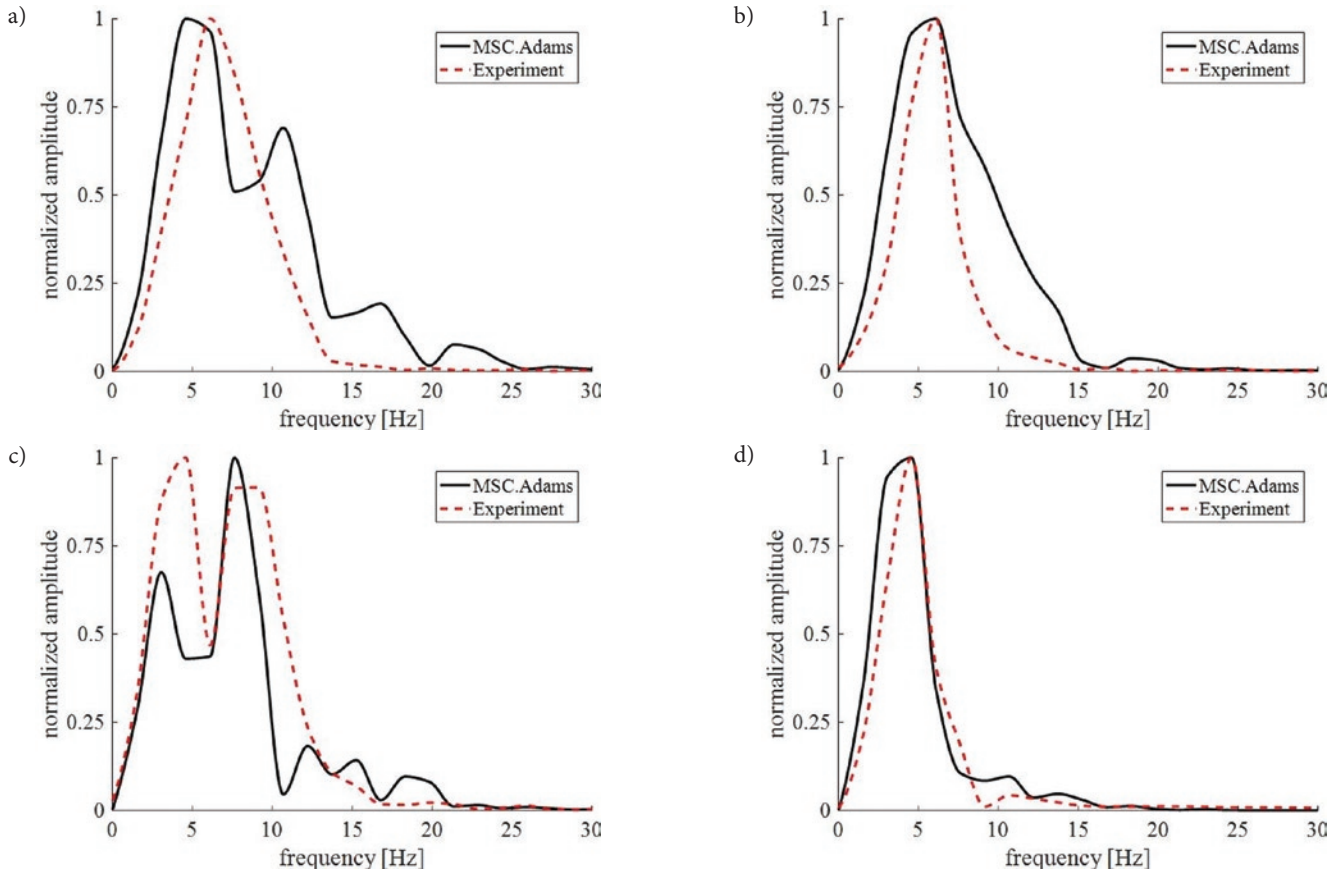
Fig. 14. Frequency response for acceleration of wheel a) and b) triangular obstacle without and with motors, c) and d) rectangular obstacle without and with motors R
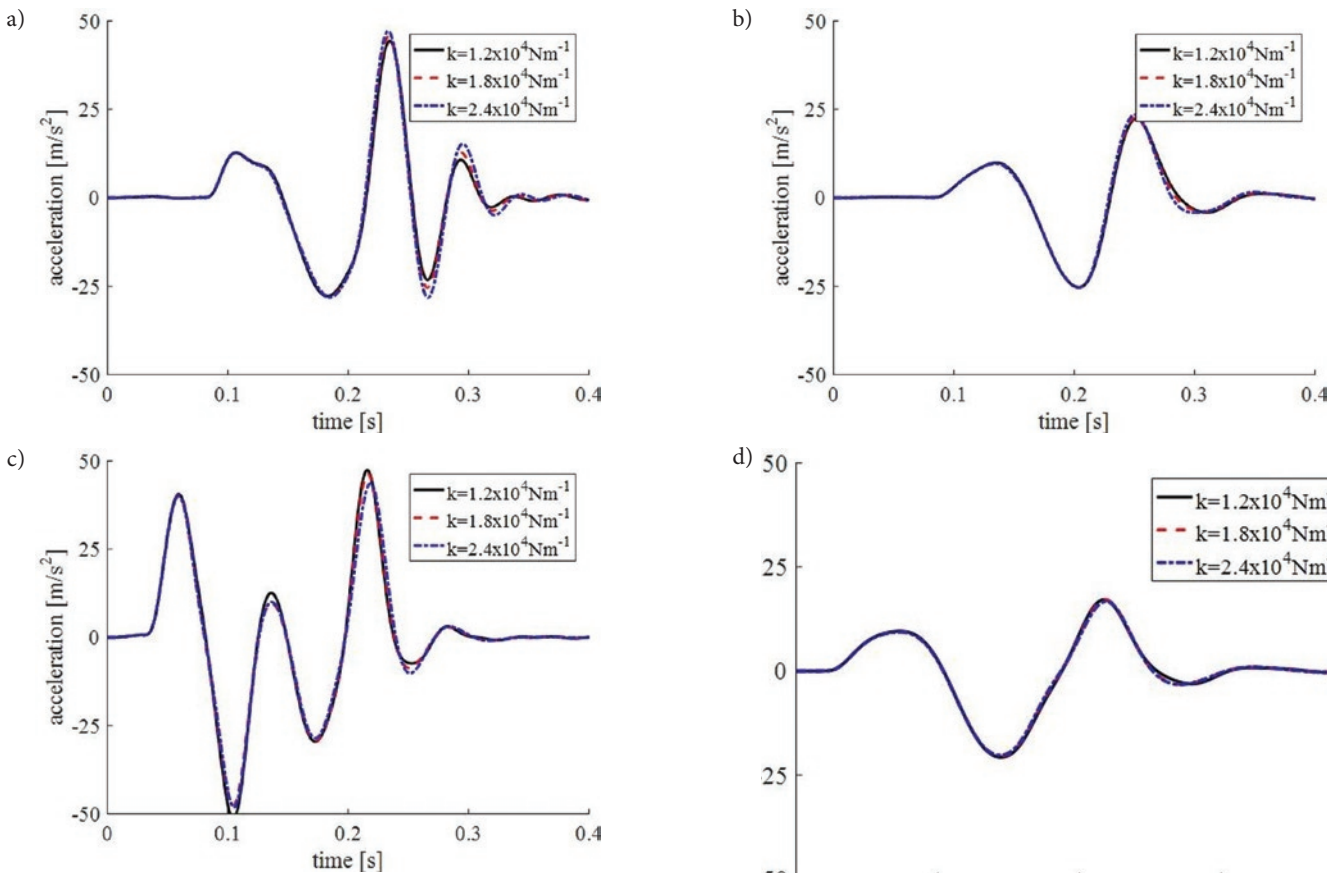

Fig. 15. Vertical acceleration of wheel for various spring stiffness values a) and b) triangular obstacle without and with motors c) and d) rectangular obstacle without and with motors
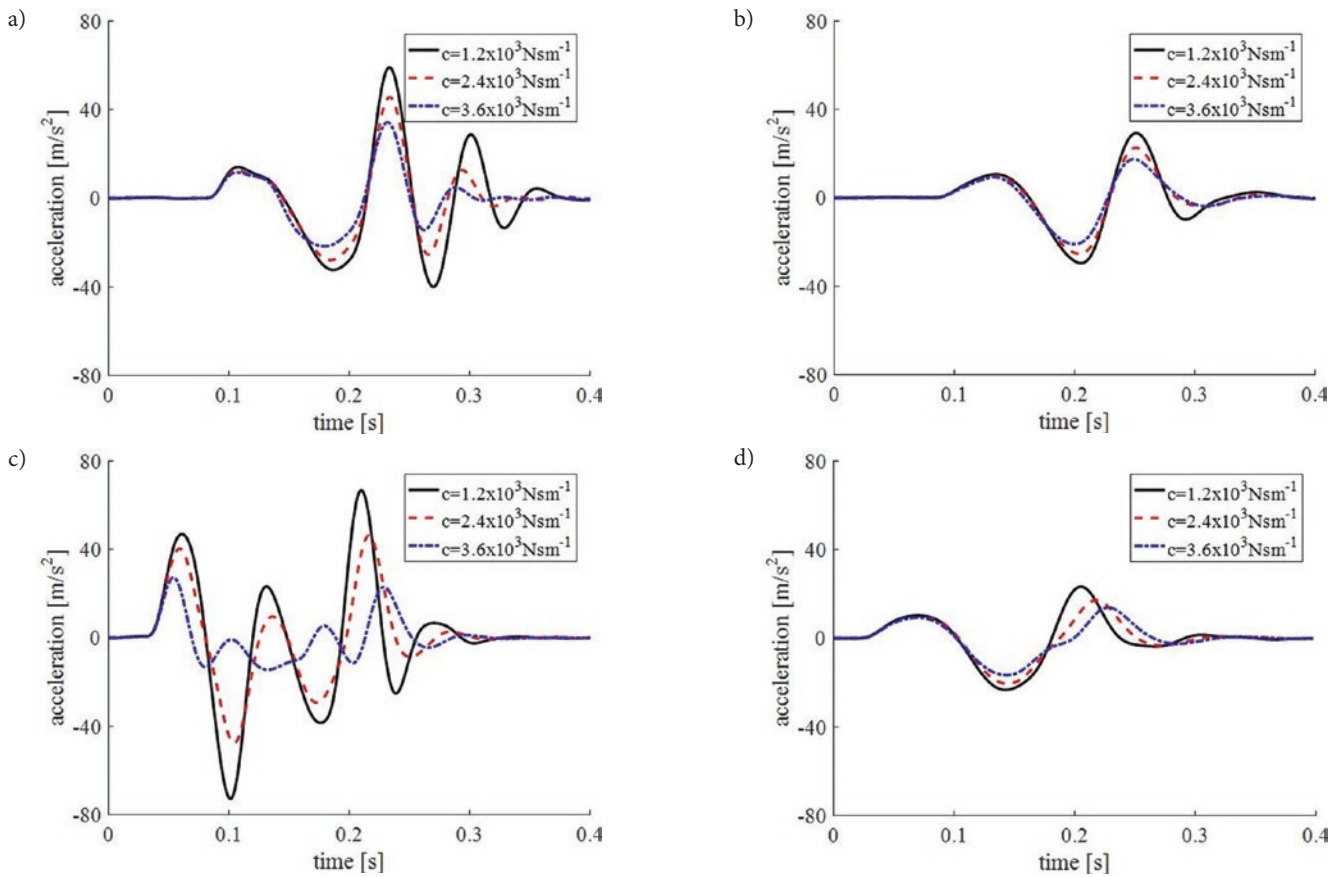
Fig. 16. Vertical acceleration of wheel for various damping coefficient values a) and b) triangular obstacle without and with motors c) and d) rectangular obstacle without and with motors
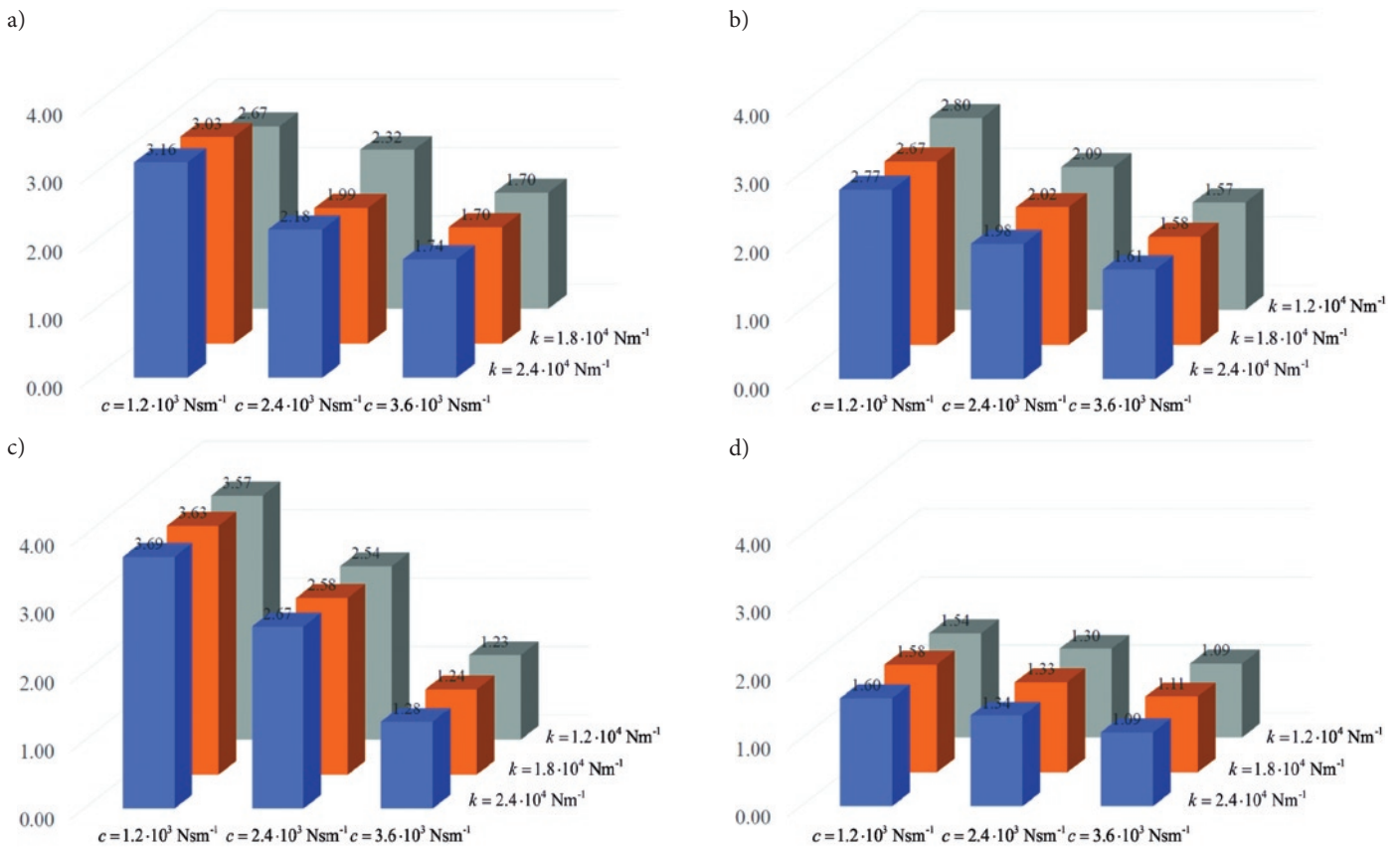

Fig. 17. RMS values a) and b) triangular obstacle without and with motors c) and d) rectangular obstacle without and with motors

a)

b)

c)

d)
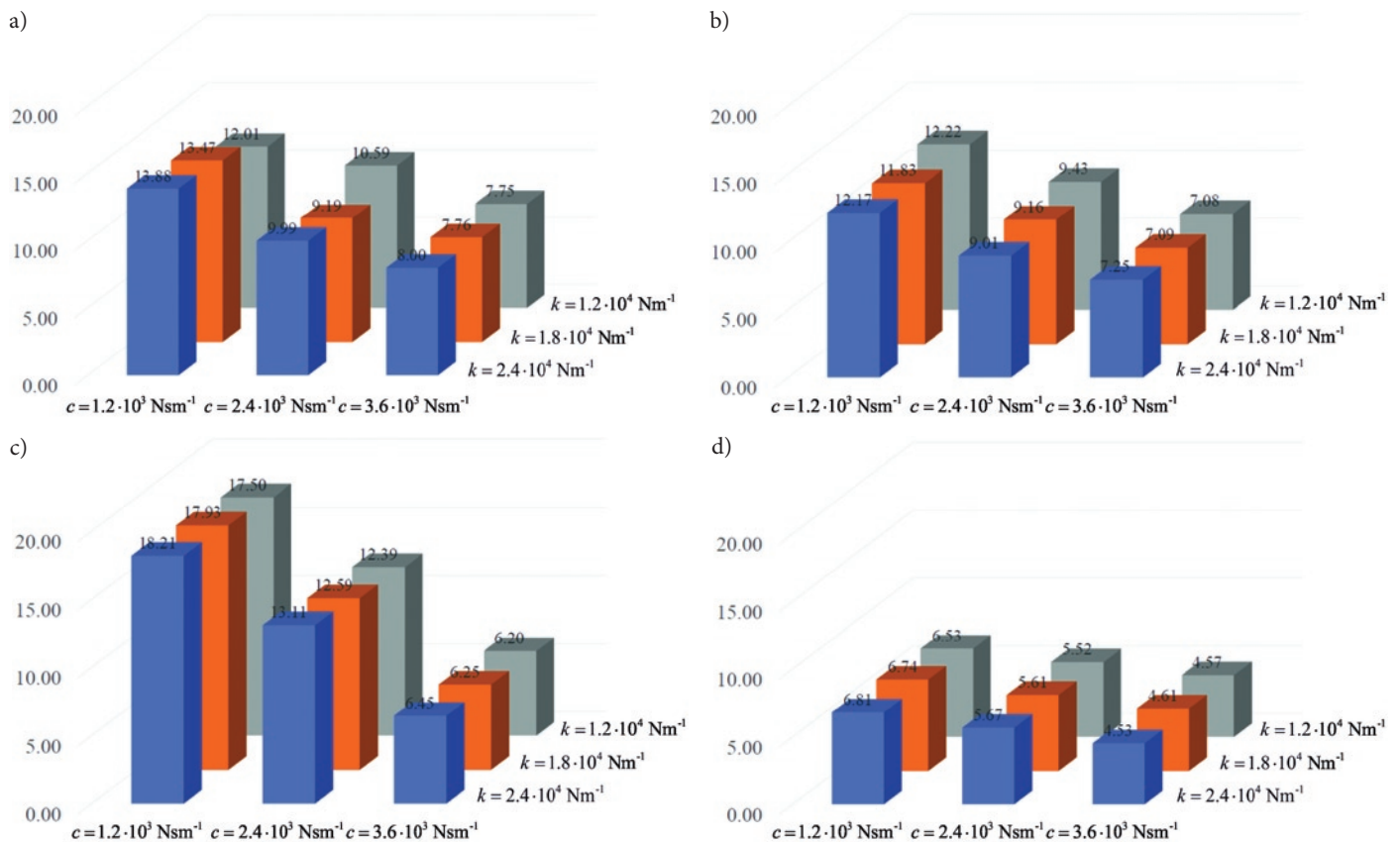

Fig. 18. VDV values a) and b) triangular obstacle without and with motors c) and d) rectangular obstacle without and with motors

courses obtained for constant spring stiffness ($k=1.8 \times 10^4$ Nm^{-1}) and variable damping coefficients.

It can be observed that the change of the spring suspension stiffness has small influence on the dynamic response of the system. Significant differences in time courses of the wheel center acceleration can be observed when the shock absorber damping coefficient is changed. It can be also noticed, that the introduction of additional mass reduces the accelerations of the wheels, which can translate into lower dynamic forces.

Values of the *RMS* and *VDV* factors obtained for an acceleration time-histories of the passenger sitting above the wheel for different spring stiffness and shock absorber damping coefficient are shown in Figs 17 and 18.

Analysing the RMS and VDV values it can be concluded that the small change of the damping coefficient significantly influence on dynamic forces acting on the rear suspension system. Only a great change in the stiffness of the suspension spring can affect the dynamic response of the system. Figure 18 shows that the installation of engines in the wheels causes a significant increase in the value of the VDV indicator from 6 to 12 for both traversed road inequalities. Although the values of this indicator are in the medium range, defined by the ISO 2631 standard, they can be reduced to a range that does not affect human health by increasing the damping in suspension.

7. Summary and conclusions

The paper presents a preliminary analysis of dynamics of the Fiat Panda III rear suspension system including electric motors mounted into wheels. The calculation model in the MSC.Adams was validated on the basis of road tests made for a vehicle without motors in wheels. On the basis of the validated model, a series of numerical calculations were performed, including motors in wheels, which were then compared with the results of the experiment. The analyses carried out

proved the high compliance of the proposed numerical model, especially for the triangular obstacle. This model was then used for further analysis of the influence of the stiffness coefficients of springs and the shock absorbers damping coefficients on vehicle dynamics.

Simplified model of the rear suspension gives good compatibility with the road test results with the experiment.

The analyses allow to state that:
- change (increase and decrease) of suspension stiffness in analyzed range slightly affects the dynamics of suspension work,
- increasing the damping in the suspension results in a significant reduction of the amplitudes of acceleration and the reduction of damping causes their increase which are confirmed by the results of tests and analyzes,
- installation of electric motors in the vehicle's wheels reduces the amplitude of displacements, velocities and accelerations of the wheel centre,
- both *RMS* and *VDV* factors obtained for the rear seat acceleration are reduced after mounting motors in wheels,
- the type of obstacle that the vehicle overcomes influences the magnitude of *RMS* and *VDV* factors and their "sensitivity" on the change of damping,

The results of the conducted simulations very closely overlap with the results of the tests on the real suspension model. The presented model can be successfully used to assess the passenger's comfort while driving.The scientific research presented in the paper was created as part of the cooperation of the Institute of Electrical Drives and Machines KOMEL and the University of Bielsko-Biala.

References

1. Anderson M, Harty D. Unsprung Mass with In-Wheel. Motors - Myths and Realities. 10th International Symposium on Advanced Vehicle Control. Loughborough, UK, 2010: 261-266.
2. Bernatt J, Król E. Comparison of two versions of electric motors used in a drivetrain of an electric car. The 25th World Battery, Hybrid and Fuel Cell Electric Vehicle Symposium & Exhibition, EVS-25 Shenzhen, China, Nov. 5-9, 2010.
3. Chłopek Z. Research on energy consumption by an electrically driven automotive vehicle in simulated urban conditions. Eksploatacja i Niezawodnosc - Maintenance and Reliability 2013; 15(1): 75-82.
4. Dixon J C. Suspension Geometry and Computation, Willey, Chichester 2009, .https://doi.org/10.1002/9780470682906
5. Dukalski P, Będkowski B, Wolnik T, Urbaś A, Augustynek K. Założenia projektu silnika do zabudowy w piaście koła samochodu elektrycznego. Maszyny Elektryczne - Zeszyty Problemowe; 2/2017 (114): 263-272.
6. Dzida J. Porównanie różnych sposobów kierunkowego napędzania pojazdów silnikami elektrycznymi. Napędy i Sterowanie 2017; 2: 50-55.
7. Ehsani M, Gao Y, Gay S E, Emadi A. Modern Electric, Hybrid Electric and Fuel Cells Vehicles, Fundamentals, Theory and Design. CRC Press; London 2017: 99-116.
8. Griffin M J. Handbook of Human Vibration, Academic Press, London 1990.
9. Król E, Rossa R. Modern magnetic materials in permanent magnet synchronous motors IEEE Xplore: 25 October 2010, 10.1109/ICELMACH.2010.5607962.
10. Kropáč O, Múčka P. Shapes of obstacles in the longitudinal road profile. Shock and Vibration 2011; 18: 671–682, https://doi.org/10.1155/2011/150487.
11. Kulkarni A, Ranjha S A, Kapoor A. A quarter-car suspension model for dynamic evaluations of an in-wheel electric vehicle. Proceedings of the Institution of Mechanical Engineers, Part D: Journal of Automobile Engineering 2018; 232(9): 1139-1148, https://doi.org/10.1177/0954407017727165.
12. Merkisz J, Pielecha I. Układy elektryczne pojazdów hybrydowych. Wydawnictwo Politechniki Poznańskiej, Poznań 2015; 12(19): 139-154
13. Pacejka H B. Tire and vehicle dynamics, SAE, Warrendale 2006.
14. Parczewski K, Wnęk H. Impact of tire inflation pressure during overcoming of road unevenness. Proceedings of 21th International Conference Transport Means. Kaunas, Part 1; 2017: 154-157.
15. Ślaski G, Gudra A, Borowicz A. Analysis of the influence of additional unsprung mass of in-wheel motors on the comfort and safety of a passenger car. The Archives Of Automotive Engineering 2014; 3(65): 51-64.
16. Watts A, Vallance A, Fraser A, Whitehead A. Integrating In-Wheel Motors into Vehicles - Real-World Experiences. SAE Int. J. Alt. Power 2012; 1(1): 289-307, https://doi.org/10.4271/2012-01-1037.
17. Wicher J., Więckowski D. Influence of vibrations of the child seat on the comfort of child's ride in a car. Eksploatacja i Niezawodnosc - Maintenance and Reliability 2010; 48(4): 102-110.
18. Zegelaar P W A. The dynamic response of tyres to brake torque variations and road unevenness's, PhD Thesis Delft University of Technology, Delft 1998.
19. ISO 2631-1:1997 Mechanical vibration and shock - Evaluation of human exposure to whole-body vibration - Part 1: General requirements. International Organization for Standarization, 1997.

Piotr DUKALSKI
Bartłomiej BĘDKOWSKI,
Institute of Electrical Drives and Machines – Komel
al. Roździeńskiego 188, 40-203 Katowice, Poland

Krzysztof PARCZEWSKI
Henryk WNĘK
Department of Combustion Engines and Vehicles
University of Bielsko-Biala
ul. Willowa 2, 43-309 Bielsko-Biala, Poland

Andrzej URBAŚ
Krzysztof AUGUSTYNEK
Department of Mechanical Engineering Fundamentals
University of Bielsko-Biala
ul. Willowa 2, 43-309 Bielsko-Biala, Poland

E-mails: p.dukalski@komel.katowice.pl, b.bedkowski@komel.katowice.pl,
kparczewski@ath.bielsko.pl, dwnek@ath.bielsko.pl, aurbas@ath.bielsko.pl,
kaugustynek@ath.bielsko.pl